

Destructive testing and computer modeling of a scale prestressed concrete I-girder bridge

Cameron D. Murray^{a,*},¹ Mauricio Diaz Arancibia^b, Pinar Okumus^b, Royce W. Floyd^a

^a School of Civil Engineering and Environmental Science, The University of Oklahoma, 202 W. Boyd St., Room 334, Norman, OK 73019-1024, USA

^b Department of Civil, Structural and Environmental Engineering, University at Buffalo, The State University of New York, 222 Ketter Hall, Buffalo, NY 14260-4300, USA

ARTICLE INFO

Keywords:

Bridges
Prestressed concrete
Shear
Distribution factors
Two-way slab
Destructive

ABSTRACT

Currently, there is a limited amount of published information on failures of prestressed concrete bridges subjected to shear and moment. A scale prestressed concrete bridge was constructed to investigate the ultimate behavior of the bridge with particular focus on load distribution after cracking and on contribution of full-depth diaphragms to structural capacity. A point load was applied at the quarter-span point of the bridge over an interior girder. As the loaded girder failed, the diaphragm-girder connection cracked. Torsion was observed to cause cracking in the exterior girder and the end diaphragm rotated away from the bridge as the deck deformed. A punching shear failure ended the test, however damage indicative of two-way slab behavior was observed in the deck. This failure suggests that post girder failure, the diaphragms provide an important means of load transfer, allowing moment redistribution in the deck and potentially increasing capacity. Testing in the elastic range compared favorably with respect to deflections and shear distribution factors from a grillage model, a 2-D finite element model and a 3-D finite element model.

1. Introduction

There is very little published literature on the ultimate behavior of bridges as a structural system [1,2,3,4,5,6,7,8]. In particular, few tests of prestressed concrete girder and slab bridges have been performed despite this bridge type being extremely common across the United States. Information about failure mechanisms in bridges can provide important guidance to designers and can improve computer modeling techniques to more accurately represent bridge behavior. Since bridges are complex systems, there is no substitute for actual load tests to failure to verify calculations of individual component capacity. A review of concrete bridge tests performed around the world determined that shear failures were particularly hard to predict, non-structural elements (like diaphragms) often contribute to capacity, and that there were fewer tests of prestressed concrete girder bridges than reinforced concrete bridges [9].

This paper details the construction and testing to failure of a roughly half length-scale prestressed concrete girder bridge. The primary goal of the scale bridge testing was to investigate shear behavior of the bridge system with particular attention paid to load distribution and behavior of the middle and end diaphragms. The effects of diaphragms on shear

behavior have not been studied extensively and there is conflicting information in the research on their effects on load distribution and behavior at ultimate loads [1,10,11,12,13]. In addition to the bridge test, 2-D and 3-D computer models were built with a goal to determine elastic shear distribution factors (DFs) and compare them with factors derived during bridge testing. Some guidance on developing bridge models to find DFs are given.

The scale bridge was composed of four roughly half-scale American Association of State Highway and Transportation Officials (AASHTO) Type-II prestressed bridge girders with a half-scale deck and full-depth diaphragms at the ends and mid-span. The scale bridge was based on a decommissioned bridge in Tulsa, OK, described in detail in a dissertation by the first author [14]. This bridge was part of a larger study on shear load rating of older bridges. A particular focus of the study was looking at the residual strength of older prestressed concrete girders when corrosion damage was present. To accomplish this task, two girders were taken from separate spans of the bridge in Tulsa and were tested in the laboratory. These girders had differing levels of prestress force and different lengths. These component tests, however, cannot provide any information about how the connectivity of several girders in a bridge system affects the overall capacity and behavior at failure of

* Corresponding author.

E-mail addresses: cdmurray@uark.edu (C.D. Murray), mdiazara@buffalo.edu (M. Diaz Arancibia), pinaroku@buffalo.edu (P. Okumus), rfloyd@ou.edu (R.W. Floyd).

¹ Present address/affiliation: Department of Civil Engineering, University of Arkansas, 4183 Bell Engineering Center, Fayetteville, AR 72701, USA.

a prestressed concrete bridge. For this reason, a scale bridge was constructed to roughly emulate the full-scale sections. The location chosen for testing the scale bridge was the quarter-span point, taken as the critical section for shear in the 11th edition of the American Association of State Highway Officials (AASHTO) Standard Specifications for Highway Bridges section 1.6.13 [15]. This location is far enough into the span that there are substantial moments and shear forces, similar to the full-scale component tests. This location also allows observations of the effects of the diaphragms and deck. Previous work has generally not considered how full depth diaphragms affect the ultimate load behavior of the bridge, but has mostly focused on contribution to load distribution [1].

Because previous work on load distribution suggests that computer models may be more accurate for calculating shear DFs than the traditional DF equations [1,11], three computer models of varying complexity were constructed to compare to the response of the scale bridge. The main goal of these models was to compare shear DFs between the scale bridge and the models since DFs determine the amount of demand assigned to a particular girder during design and load rating. AASHTO equations for DFs have been shown to be conservative for most bridges in a variety of studies [11], therefore a simple computer method, if effective, could provide a more accurate and rational estimate of load distribution. Comparing test results to models of varying complexity levels can also provide an assessment to the degree of accuracy each modeling technique offers. The models shown in this paper are a simple 2-D grillage model using frame elements only, a 2-D finite element model (FEM) using shell and frame elements, and a detailed 3-D FEM with solid elements for the concrete and truss elements for the steel reinforcement. Grillage models have been shown to be an effective way to model load distribution in girder and slab bridges [1,11]. Grillage models may be a simple replacement for DF equations that are approximate and empirical.

In addition to girders cast for inclusion in the scale bridge, scale individual girder sections were tested as part of this study [16], one of these tests provided a comparison to the behavior of the bridge system as a whole. This is described in more detail later in the paper.

2. Methods

Methods for design and construction of the scale bridge will be followed by details about the different computer models used in this study.

2.1. Scale girders and bridge

The main prestressed reinforcement in the scale girders was designed to be roughly similar to the full-scale girders from the decommissioned bridge by ensuring an in-service compressive stress from the prestress to be within 1% of that in the decommissioned girder. The decommissioned bridge and scale bridge both had the same girder cross sections across the bridge width. The shear steel was designed by using an equivalent percent contribution of the concrete and steel to the overall shear capacity. The scale I-girders were 572 mm in depth and contained two straight grade 1860–13.2 mm prestressing strands tensioned to a jacking stress of 1282 MPa. The strands were located at a distance of 102 mm from the bottom of the girder (Fig. 1). Shear reinforcement consisted of grade 420 - No. 10 Z-bars. These Z-bars also provided interface reinforcement, ensuring composite action with the bridge deck, as in the decommissioned sections. The prestressed girders were 5.49 m long and were placed at a spacing of 1.17 m (based on half the spacing provided in the full-scale bridge). The girder concrete achieved an average compressive strength at release of 30 MPa, and an average final (28-day) compressive strength of 44 MPa. These strengths are roughly similar to the strengths from the decommissioned girders, no efforts were made to scale material properties.

All girders were cast using the prestressing bed at Fears Structural

Engineering Laboratory at the University of Oklahoma. Elastomeric bearing pads were used for all supports, consistent with bridge construction in Oklahoma. The bearing pads were placed flush with the ends of the girders creating a 5.33 m span measured center to center of the pads or a 5.18 m measured face to face of the pads (the pads were approximately 160 mm wide). The bridge girders were laid out, then formwork for the deck and diaphragms was built onto the girders, such that the prestressed girders supported the full dead weight of the deck and diaphragms. The deck was 10.8 cm thick and 4.0 m wide, creating a 0.3 m overhang on each side. Diaphragms were 10.2 cm wide, began at the slab soffit and terminated 15.2 cm from the bottom of the girders. These dimensions are all half those shown on the original plans for the full scale bridge. Diaphragms were cast monolithically with the deck and a No. 13 rebar connected the interior girders with the diaphragm, while a 13 mm threaded rod embedded in the concrete attached to the exterior girders with a nut and washer. Reinforcement in the deck and diaphragms was based on the full-scale bridge, generally using about half the area of steel in the full scale bridge. Fig. 2 shows the steel used in the deck and diaphragms.

Photos from bridge construction are shown in Fig. 3. Two companion girders with a section of deck equal to the top flange width of girders were also built. This size of deck section was selected to match one of the decommissioned girders. The strength of one of these companion girders is compared to the theoretical strength of one of the scale bridge's girders later in the paper. It is worth noting here that the difference in flexural strength between the individual companion girder as cast and the strength of a girder with the tributary width of slab is only 7 percent. These girders were designed in the same fashion as the girders used in the scale bridge and one was tested with a load applied at the same location as the scale bridge, providing a comparison between the behaviors of an individual girder and the composite bridge. The deck concrete reached an average 28-day strength of 29 MPa.

The scale bridge was tested to failure at the quarter-span point over an interior girder. The quarter-span point (1.37 m from end) was chosen to facilitate comparison to one of the full-scale tests and because in previous editions of the bridge specifications, this location was taken as the critical section for shear [15]. This location has a relatively large shear and moment occurring at the same section for a typical simply supported bridge. The naming convention for the bridge girders and the load point are shown in Fig. 4. In the current AASHTO LRFD Bridge Design Specifications section 5.7.3.2, the critical section for shear is closer to the support [17]. At this location the governing load case was shear in the web, however the load location was within the transfer length of the prestressing strands, which was expected to influence the failure mechanism.

A series of elastic tests were performed to simulate service level loading followed by loading to failure. Bearing deflections were measured at all supports using linear voltage differential transformers (LVDTs). Girder deflections were also measured in line with the load point under all girders using LVDTs for elastic level deflection and wire potentiometers (pots) for larger deflections. Load was monitored using a 450 kN capacity load cell at the load point. A 20.3 cm square, 25.4 mm thick steel plate leveled with sand was used to apply load. Dial gauges were used to measure strand slip for each beam at the end being tested.

First, load was applied to the exterior girder (A) up to 89 kN. This load was selected to ensure no cracking occurred prior to the destructive test. Once several tests were performed at girder A, load was moved to girder B (interior girder). The bridge was loaded continuously to failure at this location. After the test, the initial linear portion of the load-deflection curves for all girders were considered the "elastic" loading range, and were used for comparison to computer models and to calculate DFs. This change in slope of the load deflection curve occurred at roughly 178 kN of applied force, corresponding to cracking of the loaded girder. For the destructive test, load was applied in 22 kN increments prior to cracking, followed by 8.9 kN increments, to

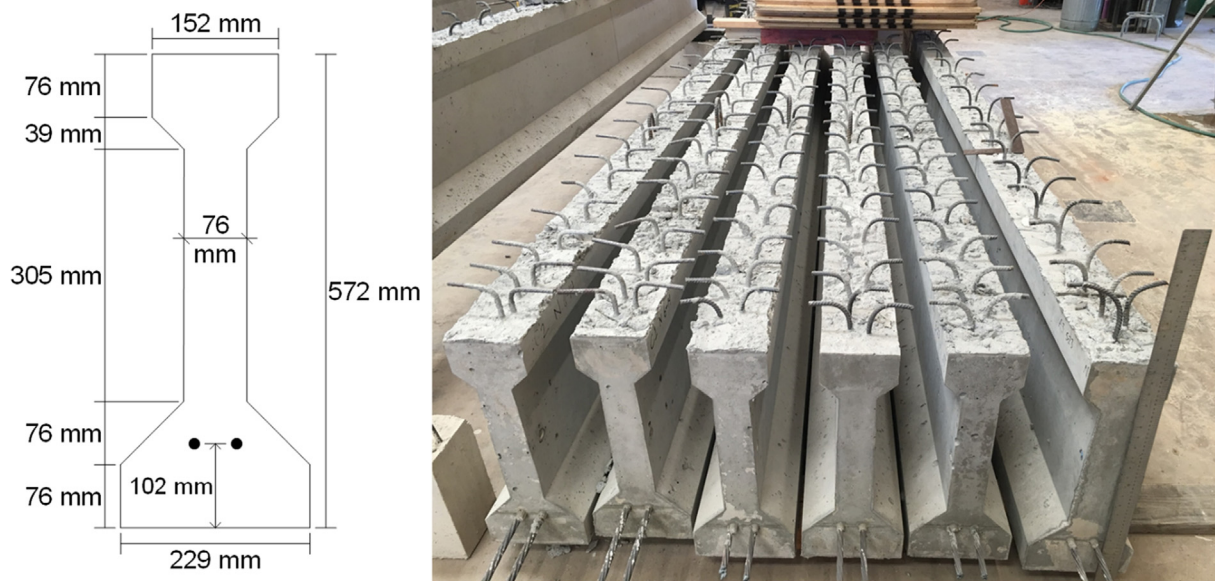


Fig. 1. Scale girder dimensions (left) and completed sections (right).

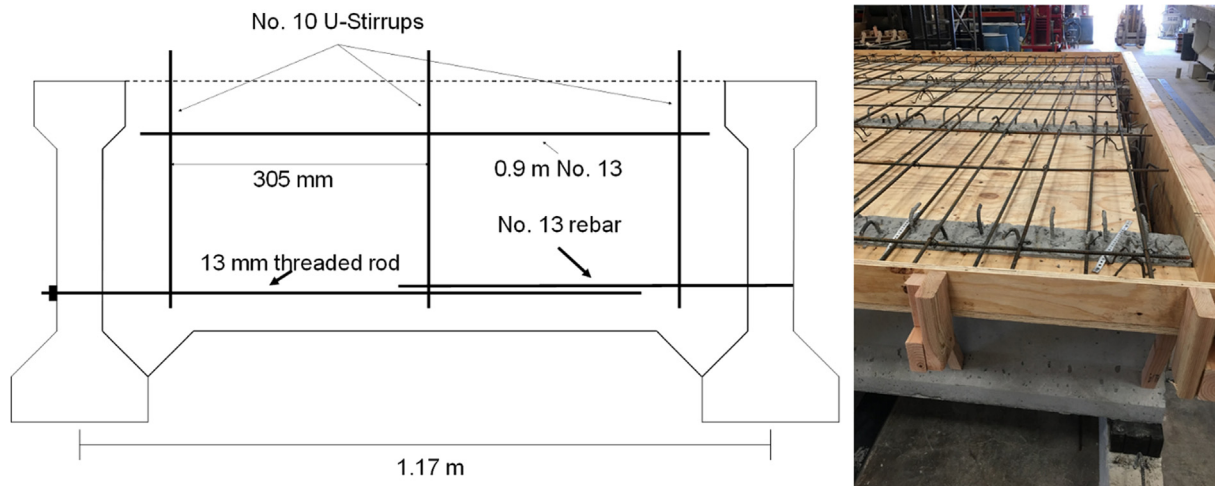


Fig. 2. Diaphragm steel (left) and deck steel (right).

facilitate tracking and marking of cracks. This same regime was used to test the individual girder specimens. More information about the test set up can be found in a dissertation by the first author [14].

2.2. Simple 2-D grillage model

A linear 2-D grillage model of the scale bridge was created using measured concrete material properties from the scale bridge. A grillage model consists of two-node frame elements in a 2-dimensional grid. The frame elements were placed at locations of strength (girders and diaphragms), and were also used to discretize the deck. The grillage model was built using guidance from Hambly [18] and O'Brien and Keogh [19] and the model was similar to other work in the literature [20]. A modular ratio was used to account for material property differences between the deck and the girders when determining grillage member cross-section properties. The grillage discretized the deck into 1/8th strips that ran parallel to bridge transverse direction, and these strips included the stiffness of the diaphragms at the ends and mid-span. Gross section properties of the girders were used including a tributary width of slab equal to the girder spacing for the interior girders and one-half the girder spacing plus the overhang for the exterior members. Pin and

roller supports were used in the grillage model.

Stiffness of the elastomeric bearing supports was derived based on deflections at the supports measured during testing and was included in the grillage model parameters. In order to compare the response of the scale bridge model with the test data, point loads of 89 kN and 178 kN were placed on girders A and B at the quarter-span point, respectively. These loads correspond to the maximum load on girder A during elastic testing (89 kN) and the linear portion of the destructive test when load was placed on girder B (178 kN). To determine shear DFs from the grillage model, reactions at each support were divided by the sum of the total reaction at that end of the bridge. This procedure has been used in similar research [21]. Shear DFs were determined from the scale bridge test in a similar way but by dividing the support deflection under each girder by the sum of the support deflections at that end of the bridge. This method seemed to provide reasonable estimates of load distribution since all supports had the same stiffness and supports are expected to behave linearly in this load range. The grillage layout is shown in Fig. 5(a).



Fig. 3. Bridge construction progress. Top left shows girders laid out and beginning of formwork construction. Top right shows completed formwork including diaphragms. Bottom left shows deck steel. Bottom right shows completed bridge with load frame.

2.3. Detailed 2-D and 3-D finite element models

Linear FEMs of the bridge tested were constructed in 2-D and 3-D using the commercial software CSiBridge [22], and Abaqus [23], respectively. The purpose of these models was to help validate the grillage model results with more complex modeling paradigms. Similar modeling techniques were used by others to analyze prestressed concrete girder bridges for load distribution [10,24,25,26] with various levels of details. The 2-D model had deck and concrete diaphragms included as four-node shell elements, while girders were introduced as two-node frame elements. The eccentricity between the deck and girder centroids was simulated by offsetting frame elements from the deck centroid. The 3-D model simulated girders, deck, and concrete diaphragms as linear hexahedral elements (solid) of type C3D8R in Abaqus. Mild and prestressing reinforcement in girders and deck were introduced as linear line elements (truss) of type T3D2 of Abaqus. The steel plate used to apply the load in the test was modeled as a discrete rigid body.

Full composite action was assumed between prestressed girders and the deck, since closely (i.e., 25 to 152 mm) spaced stirrups extending into the deck were present through the entire length of the bridge. In

the 2-D model, composite action was simulated by connecting offset nodes of frame and shell elements using “body” constraints, which causes involved nodes to move as a rigid body. In the 3-D model, composite behavior was modeled using constraints between girders and deck surfaces in contact. The constraints were “tie” type, which do not allow relative motion between contact regions. The same approach was used to represent the interaction of diaphragms with girders and deck. Mild and prestressing reinforcement, only included in the 3-D model, were embedded in concrete, constraining the translational degrees of freedom of the embedded elements to the ones of the host.

Moduli of elasticity for prestressed concrete girders were derived from average cylinder compressive strengths and using AASTHO Load and Resistance Factor Design (LRFD) provision 5.4.2.4-1 [17]. Linear interpolation was used to obtain the average compressive strengths at the time of testing. Compressive strengths ranged between 43.9 MPa and 47.3 MPa for the girders. The deck had a compressive strength of approximately 30.7 MPa. The modulus of elasticity for the concrete deck and diaphragms at testing (25.9 GPa) was predicted with ACI Committee 209 equations [27], and the 28-day average cylinder compressive strength available from testing. Concrete unit weights and Poisson’s ratio were calculated per AASHTO table 3.5.1-1 and AASHTO

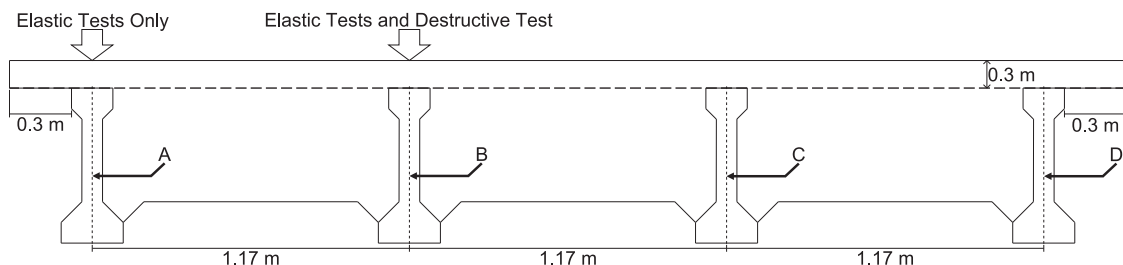


Fig. 4. Girder naming convention and location of loads.

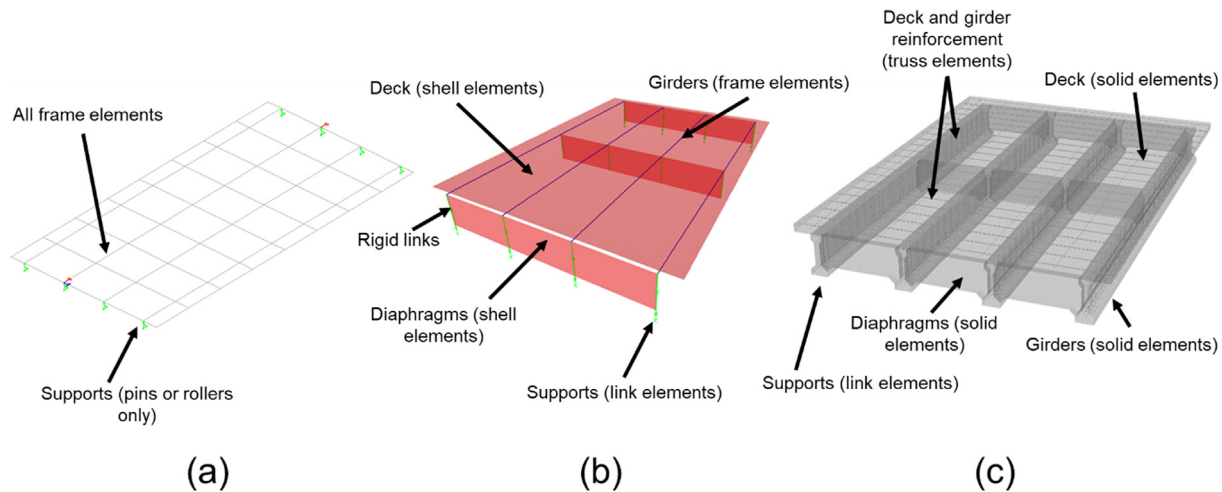


Fig. 5. Isometric view of computer models in study. (a) 2-D grillage, (b) 2-D model, (3) 3-D model.

5.4.2.5, respectively. Moduli of elasticity used for reinforcing and prestressing steel were per AASHTO 5.4.3.2 and 5.4.4.2, respectively [17]. The unit weight and Poisson's ratio used for steel were 2.39 kN/m^3 and 0.3, respectively.

The loading used in the test was modeled as a point load in the 2-D model, and as a displacement boundary condition in the 3-D model. The self-weight of all bridge components was included in both models. For simplicity, bearing pads used in the test were excluded and replaced by linear link elements, representing roller and pin supports at each end of the bridge. Prestressing was only included in the 3-D model. It was modeled by using the embedment technique [28], where strands are modeled as truss elements and embedded in concrete employing “embedded region” constraints. The jacking stress (1282 MPa) was applied as a predefined stress field, transferred at girder ends. The 2-D FEM is shown in Fig. 5(b), and the 3-D FEM is shown in Fig. 5(c).

3. Comparison of computer methods to experimental results

Tests at loads prior to cracking were performed on the scale bridge to compare to the computer models to determine if different modeling methods resulted in similar DF results. For the load over the interior girder (girder B), the deflections for all girders from the destructive test up to the cracking load of girder B (178 kN) were used for comparison. For the load on the exterior girder (girder A), the bridge was loaded up to 89 kN and then unloaded.

Fig. 6 shows the agreement between the model and the scale bridge response when load was applied at girder B (interior case). Fig. 7 shows the agreement between the models and the scale bridge response when load was applied at girder A (exterior case). Referring to Fig. 6 for the interior case, the agreement between deflections from the three computer models is good, however there are differences between the models and the bridge test. On average, when load was placed over girder B, the models differed from the test by 68 percent, or 0.120 mm. For the exterior case however (Fig. 7), the agreement between all models and the test is excellent. Deflections measured in the test differed on average from the models by only 19%, or 0.004 mm. If pinned connections were used at each support, as opposed to pin-roller connections, model results agreed better with test results where the interior girder was loaded but agreed poorly with test results where the exterior girder was loaded. Therefore, it is theorized that the discrepancy between model and test results was due to the support conditions being idealized as pin and rollers in modeling, whereas in testing elastomeric bearing pads provide intermediate restraint against rotation. Despite differences between deflections predicted by the models, DFs were considered more important to match for design or load rating purposes.

Based on the two load locations, there seemed to be an acceptable agreement between the models and the experimental results overall. It should be noted that in both cases, the differences were on the same magnitude of those observed in similar research [29].

A key comparison for this research was between DFs from the bridge testing to the three computer models. DFs used in design and load rating can have a large effect on the final design or rating factor. As stated previously, DFs for the scale bridge tests were calculated by measuring the proportion of support deflection under each girder and assuming it equal to the amount of shear at each girder. This comparison is given in Fig. 8 for the interior loading case (girder B) and Fig. 9 for the exterior loading case (girder A). The agreement between models and the bridge test appeared to be better when considering DFs compared to deflections. The most important parameter in Figs. 8 and 9 is the DF for the most heavily loaded girder. This will tend to be the controlling DF when designing or rating a bridge. For both load cases the computer models show good agreement with the measured DFs. The 2-D and 3-D detailed models differ by only 1 percent compared to the measured response for the loaded girder, for both interior or exterior girder loading cases. For the case of load over the interior girder (Fig. 8), the grillage was within 4 percent of the measured DF. On the other hand for loading over the exterior girder (Fig. 9), the grillage model significantly overestimated the DF (by 17 percent). Overall, the models seem to be adequate and conservative for predicting DFs for a bridge and may be a good alternative to the AASHTO equations. Generally, the grillage model may be a good choice for modeling bridges for load rating or design for projects that have limited computational power or for projects that require large parametric studies, as the results are generally comparable to more detailed finite element models. However, elements and properties of a grillage model should be selected with care. 2-D models provide very accurate representations of load distribution, without the assumptions needed for the grillage model and without the computational power required for 3-D models.

Figs. 8 and 9 also show the AASHTO DFs from Section 4.6.2.2.1 of the 8th edition of the AASHTO LRFD Bridge Design Specifications [17]. These DFs were included for comparison to the results of the models, but their applicability is limited for the case of this scale bridge. The scale bridge does not meet the range of applicability for the AASHTO DF equations due to the thickness of the deck and the total length of the bridge. Another issue with comparing the AASHTO DFs directly to the DFs found in this paper is that the AASHTO DFs are based on a truck loading, while the DFs in this paper are based on point loads placed directly over the girders. This difference is particularly noticeable for girder A. In Fig. 8 girder A takes less of the total shear than predicted by AASHTO because the load is based on a point load directly acting on

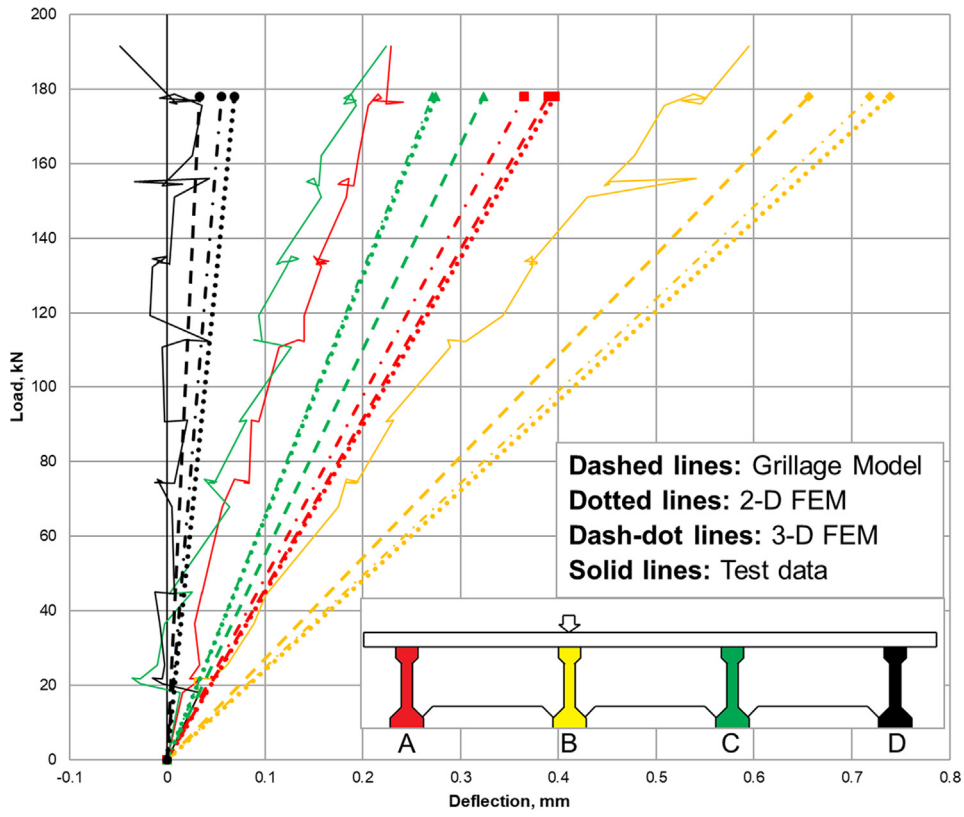


Fig. 6. Comparison of load versus deflection relationships for computer models and scale bridge loaded at girder B.

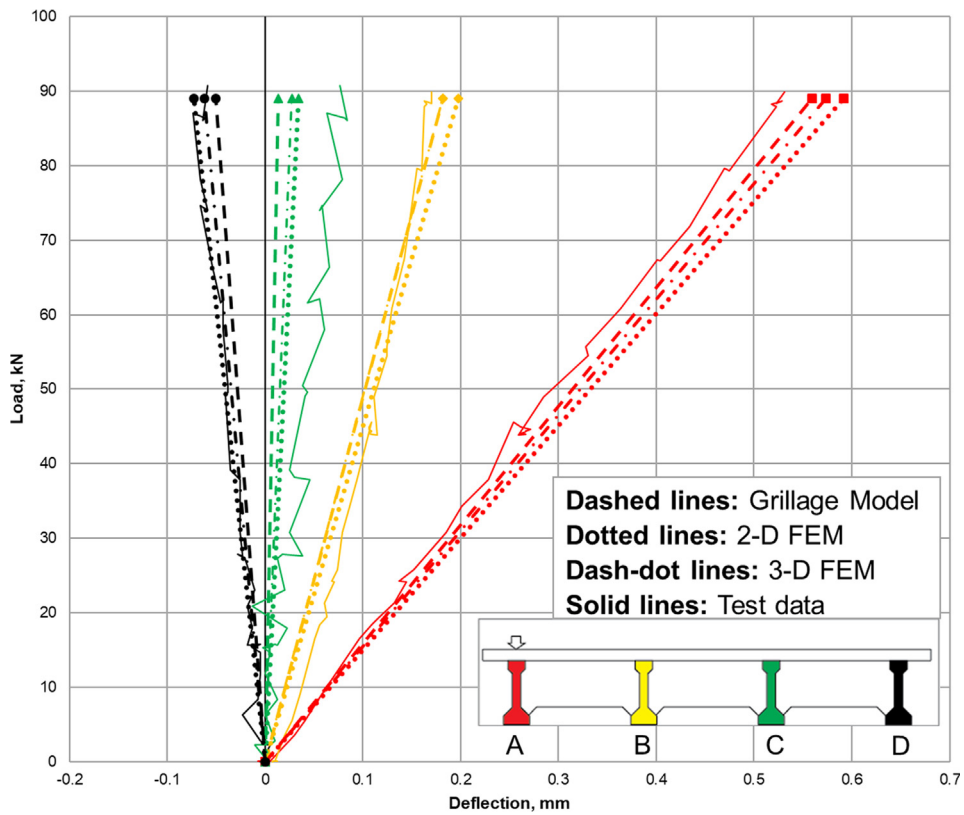


Fig. 7. Comparison of load versus deflection relationships for computer models and scale bridge loaded at girder A.

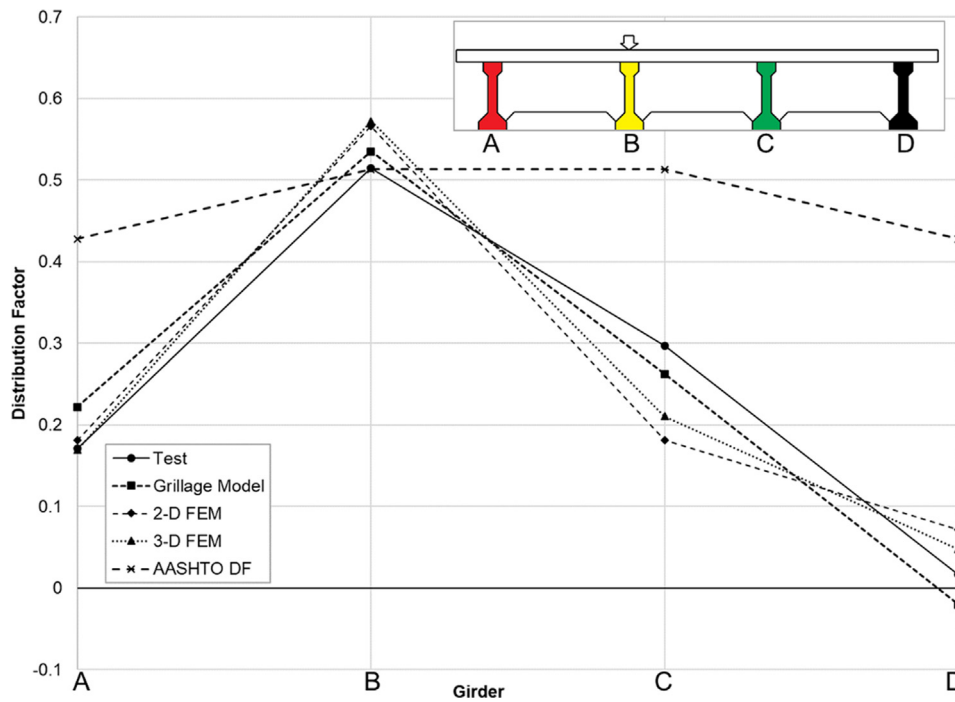


Fig. 8. Comparison of DFs from models and bridge test for interior girder (B) loaded.

girder B as opposed to the wheels of a truck. The same goes for Fig. 9 where the point load is mostly carried directly to the support of girder A instead of wheel loads that might be shared more equally between the adjacent girders.

4. Destructive testing

Destructive testing was performed to add to the limited literature on failures of prestressed concrete bridges, and to specifically investigate the contributions, if any, of the diaphragms to the shear capacity and behavior.

4.1. System test

The destructive test of the scale bridge was performed with the load over the interior girder B as shown in Fig. 4. Prior to any testing, cracking was observed at the interface between the end diaphragms and the girders. This cracking is likely due to shrinkage of the diaphragm concrete, as it was present during elastic testing, and is shown in Fig. 10. Cracking like this has been observed at bridge diaphragms in several other studies [1,13,30]. These cracks appeared to widen at early load increments, indicating some bending of the end of the bridge perhaps due to greater deflections at the support under the loaded

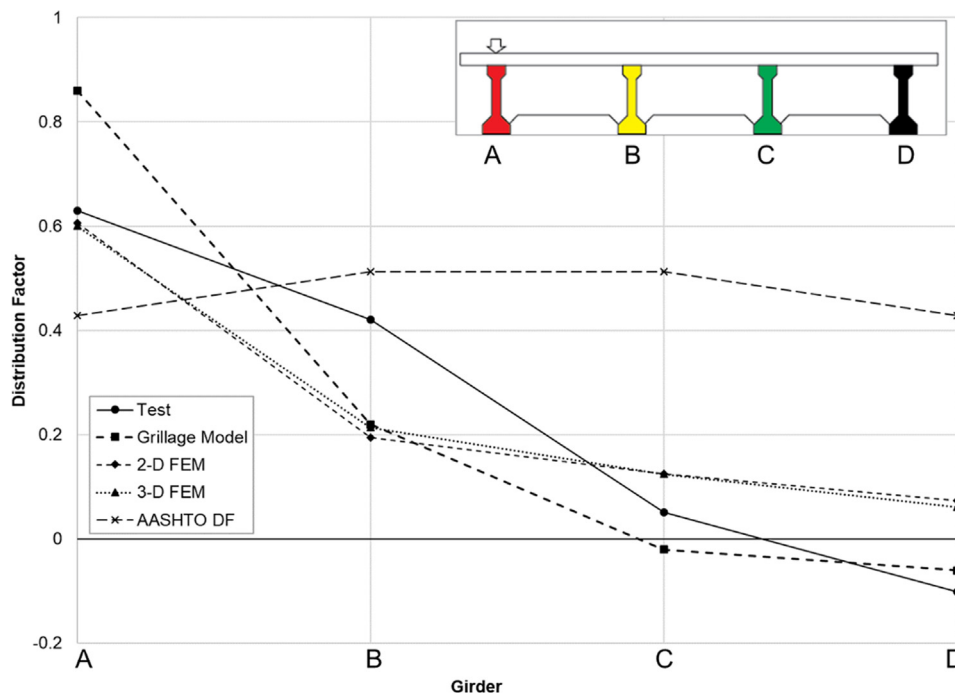


Fig. 9. Comparison of DFs from models and bridge test for exterior girder (A) loaded.



Fig. 10. Diaphragm-girder interface cracking prior to bridge test.

girder compared to the other girders.

The first visually observed girder cracking due to the applied load occurred at 245 kN. This web shear cracking occurred in the web of girder B. The slope of the load-deflection curve for this girder decreased at a load of around 178 kN, so cracking likely initiated before it was observed by the research team. At 253 kN of load, this shear cracking extended into the bottom flange of girder B interrupting the transfer length of the two 13.2 mm diameter prestressing strands in the bottom flange of the girder. At 280 kN, the first flexural crack was observed directly below the load point. Strand slip was measured in both of the strands in girder B at this time, likely related to reduced bond from the shear cracks. The measured slip for girder B is shown in Fig. 11. The dial gauges used to measure strand slip were removed at around 311 kN of load because they had reached the limit of their stroke. At 298 kN of load, another web shear crack appeared approximately 0.61 m (11%) into the span from the initial shear crack. Horizontal bond-shear cracking began to occur at a load of 334 kN and a diagonal crack on the underside of the slab appeared. This crack in the slab initiated at the load point and terminated near the corner of the slab nearest girder A. Some of the cracking in Girder B and the slab visible at 334 kN of load is

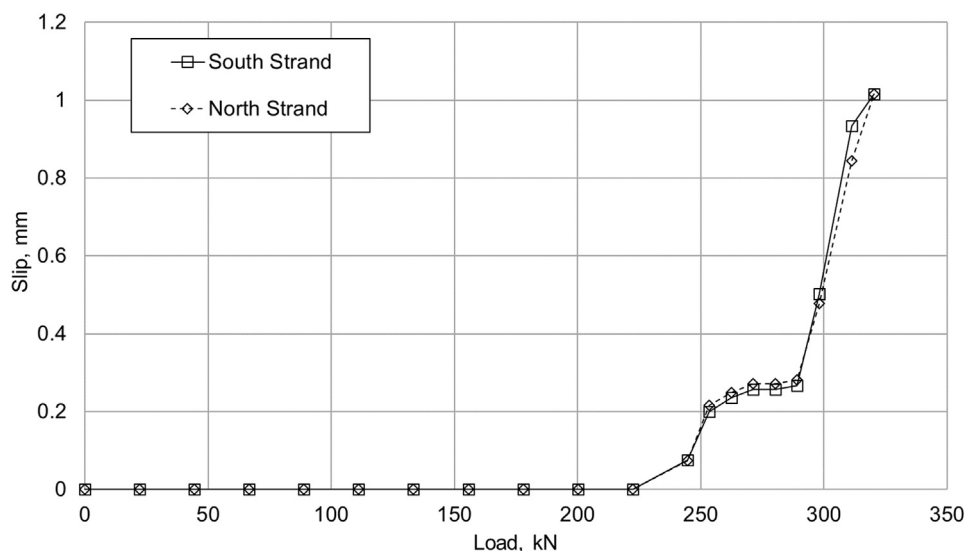


Fig. 11. Strand slip in girder B up to removal of gauges.

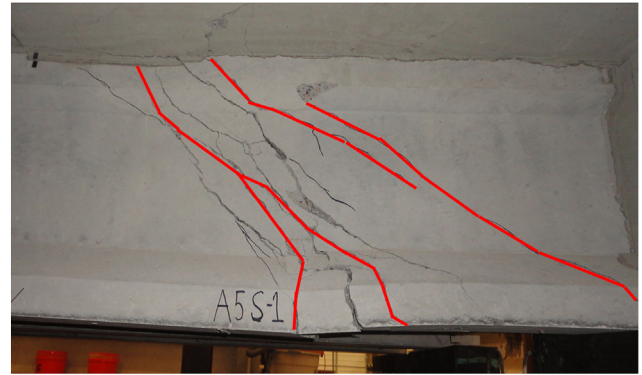


Fig. 12. Girder B final cracking (cracking at 334 kN of load outlined in red). (For interpretation of the references to colour in this figure legend, the reader is referred to the web version of this article.)

shown in Fig. 12.

At a load of 347 kN, cracking in girder A occurred at the bolted connection to the diaphragm, potentially due to limited cover between the bolt and the end of the beam. More adequate cover to the connection should have been provided, but the bolt hole spacer shifted during concrete placement. The horizontal crack at the web to flange interface on the girder indicates potential torsion in the end girder caused by the diaphragm connection. Similar cracking was also observed at the opposite end of girder A. Cracking at the diaphragm/girder interface in both ends of girders A is shown in Fig. 13. The cracking at this exterior girder appears to be related to large deformations in the deck. As girder B failed and the bridge deck deformed as a plate, girder A (exterior) rotated away from the bridge due to its connection to the deck, and the end diaphragm also rotated away from the bridge, causing the bolted connection at the girder to fail.

Load was applied up to a maximum of 427 kN, at which point there was extensive cracking in the loaded girder, including a horizontal crack at the deck-girder interface. The load point also punched through the deck at the maximum load (see Fig. 14). Punching shear was the ultimate failure mechanism for the bridge. In Fig. 14 the black arrow indicates the location of the load point. Diagonal cracking in the slab can be seen in this figure as well as large shear cracks and shear deformation in the girder. Some separation of the deck and girder occurred due to the punching shear.

Fig. 15 shows the load versus deflection curves for the destructive



Fig. 13. Cracking at diaphragm to girder connections on girder A. Left image shows end closest to load, right image shows end farther from load.



Fig. 14. Cracking in girder B at failure. Arrow indicates load location and punching shear.

test. Girder D raised off of its supports by the end of the test, as indicated by the negative deflection in Fig. 15. The change in slope of the girder B response at around 191 kN of load corresponds to initial cracking; as the cracks worsened, the deflection of the girder increased at an increasing rate. Additionally, after the loaded girder cracked, the slopes of the other girders begin to change, particularly for girder C. This is due to the additional demand on the adjacent girders when the stiffness of girder B decreased. The response of girder A (exterior) remained roughly linear for the duration of the test. The slab likely transferred more of the demand to girder C than girder A due to the larger torsional stiffness of girder C.

4.2. Individual girder test

Another shear distribution comparison was made using the results from the test of an individual scale girder. An individual girder with a

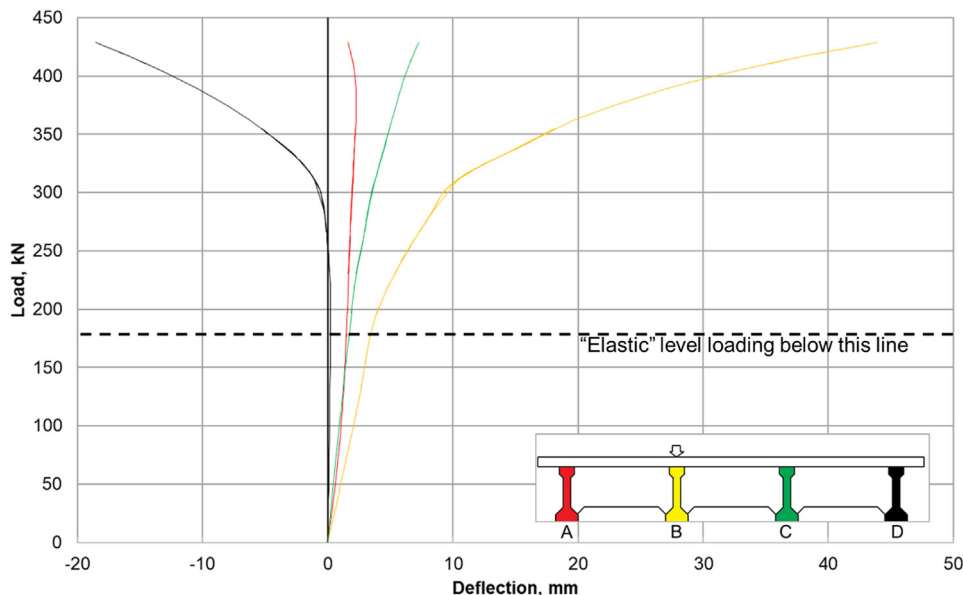


Fig. 15. Load vs. deflection for bridge test.



Fig. 16. Final cracking for individual scale girder test.

section of slab equal in width to the top flange was tested at the same load location (quarter-point). A comparison can be made between the behavior of the individual girder and the bridge system. The maximum applied load in the bridge test was 429 kN, while the maximum load in the individual test was 213 kN. This represents an increase in strength of nearly 100% upon inclusion in the bridge system. If the experimentally derived elastic DF for this girder (0.515) is multiplied by the maximum applied load in the bridge test, the resulting load for an interior girder is 221 kN. This estimated capacity for an individual section based on the ultimate load in the bridge test is 3.7% greater than the capacity measured for the individual girder. This would suggest that DFs can provide a reasonable estimate of the ultimate capacity of a bridge given the corresponding capacity of an individual girder. It should be noted that, there is only one available comparison from this research, and this comparison is for the failures influenced by a limited embedment length and significant strand slip in both the bridge and individual test. More research should be performed with other geometries, failure modes and full-scale specimens. DFs are intended to represent the amount of shear or moment in an individual girder based on the total shear or moment in the bridge at a given location. The code approach is to assume that the elastic level DFs are appropriate for estimating load distribution at ultimate loads.

A picture of the individual girder failure is shown in Fig. 16. Note that the shear cracking at the end of this girder is similar to the cracking pattern observed for the loaded girder (girder B) in the bridge test. The nominal flexural capacity of the individual girder calculated using strain compatibility was 200 kN-m compared to a calculated moment capacity of 215 kN-m for the bridge using the tributary width of the deck (7 percent difference). The capacity should theoretically have been governed by flexure in both cases, however shear cracking caused strand slip and reduced the shear capacity, leading to bond-shear failures in both cases. The shear span-to-depth ratio of this test was only 2.4, and bond-shear failures are often observed for this type of loading [31].

4.3. Discussion of deck and diaphragm behavior in bridge test

Final cracking in the bridge deck is shown in Fig. 17. A typical highway bridge deck for simply supported bridges can be designed as a one-way slab continuous over the girders. However, there are several reasons to believe the failure of the deck during this test is indicative of a two-way slab rather than a one-way slab. The deck cracking pattern suggests the failure of a two-way slab supported on its edges by the girders A and C and the middle and end diaphragms. The circular cracking visible around the load point, with negative moment cracking at the girders adjacent to the loaded girder and at the diaphragms is

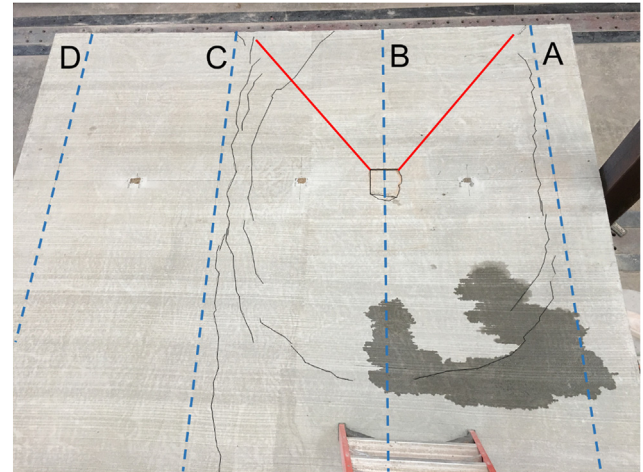


Fig. 17. Deck cracking from bridge test. Cracking visible in the deck top is highlighted in black. Dashed lines indicate locations of girders. Red lines denote locations of cracking on underside of bridge deck. (For interpretation of the references to colour in this figure legend, the reader is referred to the web version of this article.)

similar to a two-way slab with a point load in the middle. There was less negative moment cracking observed at the top of the slab at the face of the end diaphragm compared to the middle diaphragm. This diaphragm rotated away from the ends of the girders, and thus had less stiffness to resist the negative moment in the deck. The diagonal cracking underneath the deck is also similar to the assumed behavior of two-way slabs for yield line analysis. The loss in load carrying capacity of a girder (in this case the loaded girder B) resulted in a transition from one-way slab behavior to two-way slab behavior.

This shift from one to two-way slab behavior is dependent on the geometry of the bridge and the connection between the diaphragms and the deck. In a bridge with closely spaced girders and a sufficiently large distance between diaphragms, even after a girder failure, one-way slab behavior may be expected. In order for the diaphragms to act as edge beams for the deck, they must (a) be connected to the deck, and (b) be stiff enough to resist torsion due to deck deformation. Referring to Fig. 17, the cracking in the deck at the end of the bridge suggests less negative moment than the cracking at the middle diaphragm. This is due to rotation of the end diaphragms away from the bridge. Additionally, the diaphragms should be almost full depth or they must have sufficient stiffness to act as beams, transmitting load from the deck into the supports, or the adjacent girders. Because two-way slabs have greater load carrying ability than one-way slabs due to moment redistribution, one would expect greater capacities from bridges with relatively closely spaced full-depth diaphragms (two-way behavior) after a girder failure than in bridges with only partial depth diaphragms (one-way behavior). This is a potential source of redundancy that is not accounted for in design. While more work is needed to characterize this behavior, particularly with differing bridge geometries, the work presented in this paper suggests that full depth diaphragms are a prudent design choice to provide redundancy in the bridge system.

5. Conclusions

The computer models presented here provided good agreement compared to each other and compared to the results of the scale bridge test. Grillage models were computationally simple compared to the 2-D and 3-D FEMs, and appeared to be nearly as accurate. Although grillage method is the least computationally demanding modeling method of all, it requires experience, judgement, assumptions, and time from the modeler when discretizing deck into frame elements. 2-D models are computationally efficient and produce similar results to 3-D models.

Therefore, 2-D modeling is recommended in analyzing bridges. In general, models were not as accurate for predicting load distribution when the load was placed over an interior girder as when the load was on an exterior girder, however this difference is attributed to the idealized support conditions typically used in modeling.

Elastic DFs from the scale bridge test compared favorably to DFs found in computer models. Load DFs did not remain linear after cracking in the bridge for the single bridge tested in this study. More research is needed to characterize this behavior including other geometries and failure modes. Based on a test of an individual scale girder, the DFs calculated based on pre-cracking loads in the scale bridge provided a good estimate of the ultimate load the bridge could resist. This seems to back up the approach taken by the AASHTO LRFD code for strength design of bridges and bridge girders.

The results of the scale bridge test presented in this paper indicate that the presence of near full-depth diaphragms in prestressed concrete bridges can affect the failure mechanism of the bridge, potentially causing damage due to torsion in the girders and additional cracking at the girder to diaphragm connection. Despite these potential sources of damage at ultimate loads, diaphragms which are connected to the bridge deck can provide redundancy in a prestressed concrete bridge and should be chosen over partial depth diaphragms for this reason. The diaphragms serve as additional load transfer elements in the case of the failure of an individual girder. As reported in other bridge load tests, punching shear is a common failure mechanism [1,4,7,8]. This seems to be related to the relatively small areas of point loads applied during most bridge tests in research and lateral restraint of girders on the deck. Other behavior observed in the bridge deck was an apparent transition from one-way slab behavior (as designed) to two-way type behavior at ultimate loads in the presence of appropriate geometry and adequately stiff diaphragms. This two-way behavior likely helps to redistribute load in the bridge after girder failure. Additional testing is recommended to understand the behavior of diaphragms and deck near ultimate loading for a larger domain of bridges.

Acknowledgements

This research was funded by the Oklahoma Department of Transportation (ODOT). The authors wish to thank Mr. Walt Peters of ODOT for his help during this project. The authors also want to thank Mr. Mike Schmitz of the Donald G. Fears Structural Engineering Laboratory for technical support and guidance. Thanks to the Dwight D. Eisenhower Transportation Fellowship Program for funding the author during this work.

Appendix A. Supplementary material

Supplementary data to this article can be found online at <https://doi.org/10.1016/j.engstruct.2019.01.018>.

References

[1] Dymond BZ, French CE, Shield CK. Investigation of Shear Distribution Factors in

- Prestressed Concrete Girder Bridges: Minnesota Department of Transportation, St; 2016.
- [2] Jorgenson JL, Lawson W. Field testing of a reinforced concrete highway bridge to collapse. *Transport Res Record: J Transport Res Board* 1973;607(99):335–48.
- [3] Burdette EG, Goodpasture DW. Tests of four highway bridges to failure. *J the Struct Div* 1973;99:335–48.
- [4] Miller RA, Aktan AE, Shahrooz BM. Destructive testing of decommissioned concrete slab bridge. *J Struct Eng* 1994;120:2176–98.
- [5] Zhang J, Peng H, Cai CS. Destructive testing of a decommissioned reinforced concrete bridge. *J Bridge Eng* 2013;18:564–9.
- [6] Bechtel A, McConnell J, Chajes M. Ultimate capacity destructive testing and finite-element analysis of steel I-girder bridges. *J Bridge Eng* 2011;16:197–206.
- [7] Ensink S, Veen Cvd, Hordijk D, Lantsoght E, Ham Hvd, Boer Ad. In: *European Bridge Conference*, Edinburgh, Scotland; 2018.
- [8] Amir S, Cvd Veen, Walraven J, Boer Ad. Experiments on punching shear behavior of prestressed concrete bridge decks. *ACI Struct J* 2016;113:627–36.
- [9] Bagge N, Popescu C, Elfgren L. Failure tests on concrete bridges: have we learnt the lessons? *Struct Infrastruct Eng* 2017;14:292–319.
- [10] Bae HU, Oliva MG. Moment and shear load distribution factors for multigirder bridges subjected to overloads. *J Bridge Eng* 2012;17:519–27.
- [11] Mertz D. NCHRP Report 592: Simplified Live Load Distribution Factor Equations: Washington: NCHRP; 2006.
- [12] Huo XS, Wasserman EP, Iqbal RA. Simplified method for calculating lateral distribution factors for live load shear. *J Bridge Eng* 2005;10:544–54.
- [13] Cai CS, Shahawy M, Peterman R. Effect of diaphragms on load distribution of prestressed concrete bridges. *Transp Res Rec* 2002;1814.
- [14] Murray CD. *Understanding Ultimate Behavior of Prestressed Concrete Girder Bridges as a System Through Experimental Testing and Analytical Methods*. Norman, {OK}: The University of Oklahoma; 2017.
- [15] AASHTO. *Standard Specifications for Highway Bridges: American Association of State Highway Officials*, Washington, D; 1973.
- [16] Floyd RW, Pei JS, Murray CD, Cranor B, Tang PF. *Understanding the Behavior of Prestressed Girders After Years of Service: Oklahoma Department of Transportation*, Oklahoma City, {OK}; 2016.
- [17] AASHTO. *AASHTO LRFD Bridge Design Specifications*. 8th Edition: Washington, D. C; American Association of State Highway and Transportation Officials; 2017.
- [18] Hambly EC. *Bridge deck Behaviour*. CRC Press; 1991.
- [19] O'Brien EJ, Keogh DL. *Bridge deck analysis*, 1st ed., E & FN Spon; 1999.
- [20] Millam JL, Ma J. Single-lane live load distribution factor for decked precast, prestressed concrete girder bridges. *Transport Res Record: J Transport Res Board* 2005;1928:142–52.
- [21] Cross B, Vaughn B, Panahshahi N, Petermeier D, Siow YS, Domagalski T. Analytical and experimental investigation of bridge girder shear distribution factors. *J Bridge Eng* 2009.
- [22] Computers and Structures Inc. *CSiBridge 19.2*; 2017.
- [23] Dassault Systemes Simulia Corporation. *ABAQUS 6: 19-1, Johnston, {RI}*; 2017.
- [24] Barr PJ, Eberhard MO, Stanton JF. Live-load distribution factors in prestressed concrete girder bridges. *J Bridge Eng* 2001;5:298–306.
- [25] Barr PJ, Amin MN. Shear live-load distribution factors for I-girder bridges. *J Bridge Eng* 2006;11:197–204.
- [26] Idriss R, Liang Z. In-service shear and moment girder distribution factors in simple-span prestressed concrete girder bridge. *Transport Res Record: J Transport Res Board* 2010;2172:142–50.
- [27] ACI Committee 209. *209.2R-08 Guide for Modeling and Calculating Shrinkage and Creep in Hardened Concrete*; 2008.
- [28] Arab A, Badie S, Manzari A. A methodological approach for finite element modeling of pretensioned concrete members at the release of pretensioning. *Eng Struct* 2011;6:1918–2929.
- [29] Petersen-Gauthier J. Application of the grillage methodology to determine load distribution factors for spread slab beam bridges; 2013.
- [30] Dereli O, Shield C, French C. Discrepancies in shear strength of prestressed beams with different specifications; 2010.
- [31] Ross BE, Ansley M, Hamilton H. Load testing of 30-year-old AASHTO Type III highway bridge girders. *PCI J* 2011;56.